

Search for anomalous top-gluon couplings at LHC revisited

Zenro HIOKI^{1);a)} and Kazumasa OHKUMA^{2);b)}1) Institute of Theoretical Physics, University of Tokushima
Tokushima 770-8502, Japan2) Department of Information Science, Fukui University of Technology
Fukui 910-8505, Japan

ABSTRACT

Through top-quark pair productions at LHC, we study possible effects of non-standard top-gluon couplings yielded by $SU(3) \times SU(2) \times U(1)$ invariant dimension-6 effective operators. We calculate the total cross section and also some distributions for $pp \rightarrow t\bar{t}X$ as functions of two anomalous-coupling parameters, i.e., the chromoelectric and chromomagnetic moments of the top, which are constrained by the total cross section ($pp \rightarrow t\bar{t}$) measured at Tevatron. We find that LHC might give us some chances to observe sizable effects induced by those new couplings.

PACS: 12.38.-t, 12.38.Bx, 12.38.Qk, 12.60.-i, 14.65.Ha, 14.70.Dj

Keywords: anomalous top-gluon couplings, Tevatron, LHC, effective operators

^{a)}E-mail address: hioki@ias.tokushima-u.ac.jp

^{b)}E-mail address: ohkuma@fukui-ut.ac.jp

1. Introduction

The Large Hadron Collider, LHC, now being about to operate [1], we will soon be able to study physics beyond the standard model of the strong and electroweak interactions in TeV world. Studies of such new physics can be classified into two categories: model-dependent and model-independent approaches. It is of course meaningless to try to find which is more efficient: they have both advantage and disadvantage. That is, the former could enable very precise calculations and analyses, but we have to start again from the beginning if the wrong framework was chosen, while we would rarely fail to get meaningful information in the latter but it would not be that easy there to perform very precise analyses since we usually need to treat many unknown parameters together. Therefore these two approaches to new physics should work complementary to each other.

One reasonable way to decrease the number of such unknown parameters in a model-independent analysis is to assume a new physics characterized by an energy scale Λ and write down $SU(3) \times SU(2) \times U(1)$ -symmetric effective (non-renormalizable) operators for the world below Λ . Those operators with dimension 6 were systematically listed in [2]. Although we still have to treat several operators (parameters) even in this framework, but some of the operators given there were found to be dependent of each other through equations of motion [3]. This shows that we might be further able to reduce the number of independent operators, and indeed it was recently done in [4].

In this effective-operator framework, not only electroweak couplings but also QCD couplings receive nonstandard corrections. It will be hard for many readers to imagine that the QCD couplings of light quarks are affected by those anomalous interactions, since the standard QCD interaction form has so far been tested very well based on a lot of experimental data. The top-quark couplings might however be exceptional, because this quark has not been studied enough precisely yet, and its extremely heavy mass seems to tell us something about a new physics beyond the standard model. That is, the t quark could work as a valuable window to a non-SM physics once LHC starts to give us fruitful data.

Under this consideration, we would like to perform here an analysis of anomalous

bus top-gluon couplings produced by the dimension-6 effective operators through top-quark pair productions at LHC. We first describe our calculational framework in section 2. In section 3, we calculate the total cross section of $pp \rightarrow t\bar{t}X$ at Tevatron energy and compare the result with the corresponding CDF/D0 data [5], which gives a constraint on the anomalous-coupling parameters. We then use them to compute the total cross section and also some distributions for $pp \rightarrow t\bar{t}X$ at LHC, i.e., the top-angular, the top-transverse-momentum, and the $t\bar{t}$ -invariant-mass distributions. There we will find that LHC might give us some chances to observe sizable effects induced by the new couplings. Finally, a summary is given in section 4.

2. Framework

Let us clarify our basic framework in this section. In ref.[2] were given three effective operators contributing to strong interactions. Those operators produce top-pair production amplitudes which include $\bar{t}_i t_j$, $\bar{t}_i t_j$ and $\bar{t}_i t_j$ terms (or more complicated Lorentz structure), where $p_{i,j}$ and q are the top-quark i, j and gluon momenta. However two of them were shown not to be independent in [4], and we only need to take into account one operator

$$O_{uG}^{33} = \sum_a [q_{L3}^a(\mathbf{x}) \bar{u}_{R3}(\mathbf{x}) \sim(\mathbf{x}) G^a(\mathbf{x})]; \quad (1)$$

where we followed the notation of [4]. This is quite a reduction. Now the anomalous top-gluon couplings are given by

$$O_{gt} = \frac{1}{2} \frac{v}{\Lambda^2} \sum_a \bar{t}_t(\mathbf{x}) \gamma^a (1 + \gamma_5) t_t(\mathbf{x}) G^a(\mathbf{x}); \quad (2)$$

and our starting Lagrangian thereby becomes with unknown coefficients C_{uG}^{33} as

$$\begin{aligned}
 L &= L_{SM} + \frac{1}{2} [C_{uG}^{33} O_{gt} + C_{uG}^{33} O_{gt}^y] \\
 &= L_{SM} + \frac{1}{2} \frac{v}{\Lambda^2} \sum_a [\text{Re}(C_{uG}^{33}) \bar{t}_t(\mathbf{x}) \gamma^a t_t(\mathbf{x}) \\
 &\quad + i \text{Im}(C_{uG}^{33}) \bar{t}_t(\mathbf{x}) \gamma^a \gamma_5 t_t(\mathbf{x})] G^a(\mathbf{x}); \quad (3)
 \end{aligned}$$

Here v is the Higgs vacuum expectation value (≈ 246 GeV), and $\text{Re}(C_{uG}^{33})$ and $\text{Im}(C_{uG}^{33})$ correspond to the top-quark chromomagnetic and chromoelectric moments respectively.

As a matter of fact, a number of analyses including nonstandard couplings have been performed in tt productions at high-energy hadron colliders ever since more than a decade ago [6, 7]. However, the couplings used there were not always the same. The precision of CDF/D0 data used there was not that high either. In contrast to it, we can now state that the analysis using the two moments is the most general model-independent one within the framework of effective operators. Therefore, it must be worth to revisit the CDF/D0 data, to refine the constraints on the anomalous couplings, and to apply the resultant information to $pp \rightarrow ttX$ at LHC, which is about to operate.

Apart from QCD higher order corrections, $qq \rightarrow g \rightarrow tt$ process is expressed by one Feynman diagram (Fig.1), and the corresponding invariant amplitude is given by

$$M_{qq} = \frac{1}{4\hat{s}} g_s^2 \sum_a u(p_t)^a (q) v(p_t) v(q_2)^a u(q_1); \quad (4)$$

where $q = q_1 + q_2 (= p_t + p_{\bar{t}})$; $\hat{s} = q^2$, $[a]$ is the color label of the intermediate gluon,¹¹ we expressed the anomalous-coupling parameters as

$$d_V = \frac{p_{\bar{t}}}{2\sqrt{m_t}} \text{Re}(C_{uG}^{33}); \quad d_A = \frac{p_{\bar{t}}}{2\sqrt{m_t}} \text{Im}(C_{uG}^{33});$$

and we defined as

$$(q) = \frac{2i}{m_t} q (d_V + id_A \gamma_5);$$

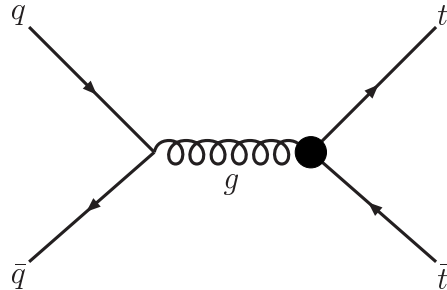


Figure 1: Feynman diagram of $qq \rightarrow tt$. The bullet expresses the vertex which includes the anomalous couplings.

¹¹Here (and hereafter) we do not show the color-component indices of u/v spinors, and also all the spin variables for simplicity.

On the other hand, $gg \rightarrow t\bar{t}$ consists of four intermediate states (Fig. 2 a,b,c,d), and the corresponding amplitudes are

$$M_{gg} = M_{gg}^a + M_{gg}^b + M_{gg}^c + M_{gg}^d;$$

$$M_{gg}^a = \frac{g_s^2}{2s_a} \bar{u}(p_t) \gamma_a v(p_{\bar{t}}) \left[\frac{1}{k_1^2} \epsilon_{\mu\nu\alpha\beta} q_{1\mu} q_{2\nu} \epsilon_{\alpha\beta} + \frac{1}{k_2^2} \epsilon_{\mu\nu\alpha\beta} q_{1\mu} q_{2\nu} \epsilon_{\alpha\beta} \right] \quad (5)$$

$$M_{gg}^b = \frac{1}{4} g_s^2 \bar{u}(p_t) \gamma_c \frac{1}{m_t} \epsilon_{\mu\nu\alpha\beta} q_{1\mu} q_{2\nu} \epsilon_{\alpha\beta} v(p_{\bar{t}}) \quad (6)$$

$$M_{gg}^c = \frac{1}{4} g_s^2 \bar{u}(p_t) \gamma_b \frac{1}{m_t} \epsilon_{\mu\nu\alpha\beta} q_{1\mu} q_{2\nu} \epsilon_{\alpha\beta} v(p_{\bar{t}}) \quad (7)$$

$$M_{gg}^d = g_s^2 \bar{u}(p_t) \gamma_a v(p_{\bar{t}}) \epsilon_{\mu\nu\alpha\beta} q_{1\mu} q_{2\nu} \epsilon_{\alpha\beta} \quad (8)$$

Here $k_1 = p_t - q_1$, $k_2 = p_{\bar{t}} - q_2$, $[a]$ and $[b; c]$ are the color labels of the intermediate gluon and the incident gluons with momenta $q_1; q_2$, $(\epsilon_{1,2})$ are the incident-gluon polarization vectors, and

$$\frac{1}{m_t} (\not{d}_V + i\gamma_5):$$

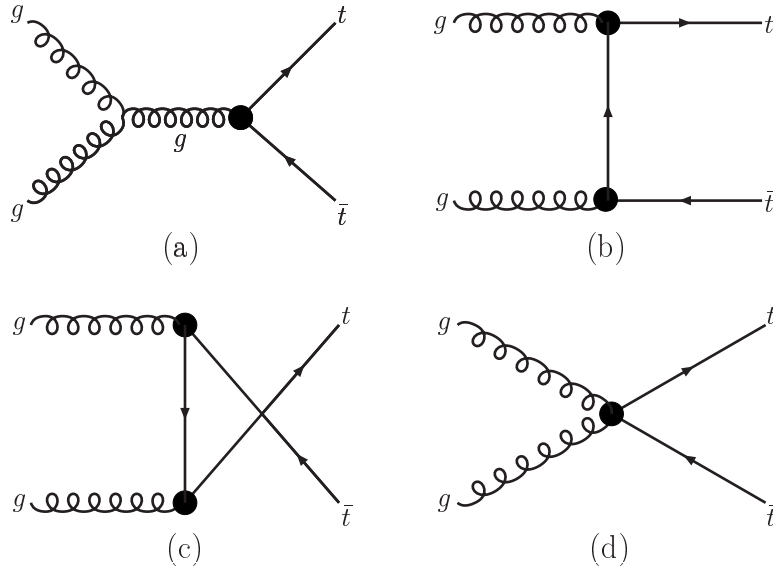


Figure 2: Feynman diagrams of $gg \rightarrow t\bar{t}$. The bullet expresses the vertex which includes the anomalous couplings.

Based on these invariant amplitudes, the differential cross sections are calculated: the one for $q\bar{q} \rightarrow t\bar{t}$ in the $q\bar{q}$ -CM frame is

$$\frac{d_{q\bar{q}}}{dE_t d\cos\theta_t} = \frac{t}{16\hat{s}} \left(\frac{P}{\hat{s}} - 2E_t \right) \frac{1}{3} \sum_{\text{color}} \frac{1}{2} \sum_{\text{spin}} \mathcal{M}_{q\bar{q}}^2; \quad (9)$$

and the one for $g\bar{g} \rightarrow t\bar{t}$ in the $g\bar{g}$ -CM frame is

$$\frac{d_{g\bar{g}}}{dE_t d\cos\theta_t} = \frac{t}{16\hat{s}} \left(\frac{P}{\hat{s}} - 2E_t \right) \frac{1}{8} \sum_{\text{color}} \frac{1}{2} \sum_{\text{spin}} \mathcal{M}_{g\bar{g}}^2; \quad (10)$$

where the asterisk was used to express that the quantities with it are those in the parton CM frame, $\beta_t = \frac{|\mathbf{p}_t|}{E_t} (= \frac{1}{\sqrt{1 + 4m_t^2/\hat{s}}})$ is the size of the produced top-quark velocity in this frame, and we already performed the azimuthal-angle integration since there is no non-trivial dependence on this angle included. After carrying out the color summation, we use the algebraic calculation system FORM [8] to evaluate $\mathcal{M}_{j\bar{j}}^2$, and perform numerical computations.

Concerning analytical expression of $\mathcal{M}_{j\bar{j}}^2$, compact formulas are found in [6, 9], which lead to

$$\sum_{\text{color spin}} \mathcal{M}_{q\bar{q}}^2 = 16g_s^4 \frac{1}{3} (1 - 2v - z) [8(d_V^2 + d_A^2) + 8(d_V^2 + d_A^2)v = z]; \quad (11)$$

color spin

$$\sum_{\text{color spin}} \mathcal{M}_{g\bar{g}}^2 = \frac{32}{3} g_s^4 (4 - v - 9) [1 - 2v + 4z(1 - z = v) - 8d_V(1 - 2d_V)]$$

$$+ 4(d_V^2 + d_A^2) [14(1 - 4d_V) = z + (1 + 10d_V) = v]$$

$$- 32(d_V^2 + d_A^2)^2 (1 = z - 1 = v - 4v = z^2); \quad (12)$$

where $z = \frac{m_t^2}{\hat{s}}$, $v = \frac{(\hat{t} - m_t^2)(\hat{t} - m_t^2 - \hat{s})}{\hat{s}^2}$, $\hat{t} = (q_1 - p_t)^2$, we have re-expressed their anomalous-coupling parameters in our notation, and the overall 4-momentum conservation has been taken into account. We confirmed that our FORM results are in complete agreement with them.

When we derive hadron cross sections from parton cross sections, we first need to connect parton cross sections in the parton-CM frame and hadron-CM frame. Among the quantities we are going to compute here, the total cross section, the top-quark p_T distribution, and the $t\bar{t}$ invariant-mass distributions are all Lorentz-transformation invariant,¹² therefore we do not have to worry about the difference

¹²Concerning the p_T distribution, note that we do not take into account the parton transverse momenta.

between these two frames. In case of the p_T distribution, we have

$$\begin{aligned} \frac{d}{dp_T} \frac{d\sigma_{q\bar{q}g}}{d\cos\theta} &= \frac{d}{dp_T} \frac{d\sigma_{q\bar{q}g}}{d\cos\theta} = \frac{Z_{c_{m\text{ax}}} d\cos\theta}{c_{m\text{in}}} \frac{d\sigma_{q\bar{q}g}}{dp_T d\cos\theta} \\ &= \frac{Z_{c_{m\text{ax}}}}{c_{m\text{in}}} d\cos\theta \frac{\dot{p}_t j}{E_t \sin\theta} \frac{d\sigma_{q\bar{q}g}}{dE_t d\cos\theta}; \end{aligned} \quad (13)$$

where the quantities without $\dot{}$ are those in the hadron-CM frame, we have chosen the z axis in the direction of q_1 so that $p_T (= p_r) = \dot{p}_t j \sin\theta$ and

$$c_{m\text{ax}} = c_{m\text{in}} = \frac{q}{1 - 4p_T^2} = \frac{p_-}{(E_t \sin\theta)^2}; \quad (14)$$

and for the $t\bar{t}$ invariant-mass distribution,

$$\frac{d}{d\sqrt{s}} \frac{d\sigma_{q\bar{q}g}}{d\cos\theta} = \frac{d}{d\sqrt{s}} \frac{d\sigma_{q\bar{q}g}}{d\cos\theta} = \frac{1}{2} \frac{d}{dE_t} \frac{d\sigma_{q\bar{q}g}}{d\cos\theta} = \frac{1}{2} \frac{Z_{+1}}{1} d\cos\theta \frac{d\sigma_{q\bar{q}g}}{dE_t d\cos\theta}; \quad (15)$$

where $\sqrt{s} = \sqrt{s} = \frac{p_-}{2E_t}$. On the other hand, we need the appropriate Jacobian connecting the two frames when the angular distribution is considered as follows: The top energy and scattering angle in the parton-CM frame are expressed in terms of those in the hadron-CM frame as

$$E_t = (E_t - \dot{p}_t j \cos\theta) \frac{q}{1 - \beta^2}; \quad (16)$$

$$\cos\theta = (\dot{p}_t j \cos\theta - E_t) \frac{q}{(\dot{p}_t j - E_t) \frac{q}{1 - \beta^2}}; \quad (17)$$

where β is the Lorentz-transformation boost factor connecting the two frames, and we used $\dot{p}_t j (= \sqrt{E_t^2 - m_t^2})$ in the denominator on the right-hand side of eq.(17) to make the formula compact. These relations lead to the Jacobian

$$\partial(E_t; \cos\theta) = \partial(E_t; \cos\theta) = \dot{p}_t j - \dot{p}_t j \quad (18)$$

and the cross-section relation

$$\frac{d\sigma_{q\bar{q}g}}{dE_t d\cos\theta} = \frac{\dot{p}_t j}{\dot{p}_t j dE_t d\cos\theta} \frac{d\sigma_{q\bar{q}g}}{dE_t d\cos\theta}; \quad (19)$$

Then the hadron cross sections are obtained by integrating the product of the parton distribution functions and the parton cross sections in the hadron-CM frame on the momentum fractions x_1 and x_2 carried by the partons. Let us explicitly show

the result of the above E_t and θ_t double distribution, since the other quantities are easier to handle:

$$\frac{d_{pp \rightarrow pp}}{dE_t d\cos\theta_t} = \sum_{a,b} \int_{4m_t^2/s}^{Z_1} dx_1 \int_{4m_t^2/(x_1 s)}^{Z_1} dx_2 N_a(x_1) N_b(x_2) \frac{\dot{p}_t^j}{\dot{p}_t^j} \frac{d_{ab}}{dE_t d\cos\theta_t}; \quad (20)$$

where $N_{a,b}(x)$ are the parton distribution functions of parton a and b ($a; b = u; \bar{u}, d; \bar{d}, s; \bar{s}, c; \bar{c}, b; \bar{b}$ and g). Thanks to the energy-conservation delta function in Eqs.(9) and (10), we can immediately perform x_2 integration and get to

$$\frac{d_{pp \rightarrow pp}}{dE_t d\cos\theta_t} = \sum_{a,b} \int_{x_{1min}}^{Z_1} dx_1 N_a(x_1) N_b(x_2) \frac{x_2^q}{(1+x_2)(1-x_2 \cos\theta_t)} \frac{1}{8 \hat{s} \hat{s}} \frac{1}{f_c} \sum_{color} \frac{1}{f_s} \sum_{color} \mathcal{M}_{ab}^j; \quad (21)$$

where $\theta_t = \angle(\dot{p}_t, \dot{E}_t)$, $\hat{s} = (x_1 - x_2)E_t = (x_1 + x_2)E_t$, \hat{s} is related to s defined via the hadron momenta $p_{1,2}$ ($s = (p_1 + p_2)^2$) as $\hat{s} = x_1 x_2 s$, f_c and f_s are the color and spin degrees of freedom of the incident partons respectively, and x_2 is now given as

$$x_2 = \frac{x_1 E_t (1 - \cos\theta_t)}{x_1 \hat{s} E_t (1 + \cos\theta_t)}; \quad (22)$$

Since x_1 and x_2 must satisfy $4m_t^2/(x_1 s) \leq x_2 \leq 1$, we have

$$x_{1min} = \frac{E_t (1 + \cos\theta_t)}{\hat{s} E_t (1 - \cos\theta_t)}; \quad (23)$$

The top angular distribution is obtained by integrating eq.(21) on E_t over

$$m_t \leq E_t \leq \frac{\sqrt{s}}{2};$$

3. Analyses

We are now ready to perform numerical computations. We first compare the total cross section of $pp \rightarrow t\bar{t}X$ at Tevatron energy with CDF/D0 data to get improved constraints on $d_{V,A}$, then compute the total cross section, the top angular distribution, the top p_T distribution, and the $t\bar{t}$ invariant-mass distribution of $pp \rightarrow t\bar{t}X$ at LHC energy. Those top cross sections are not a quantity which directly shows the CP nature of the interactions, and therefore depend both on $d_{V,A}$. This may seem inefficient but we could thereby get useful information of both parameters at the same time.

3.1. Analysis of Tevatron data

The latest data of tt pair productions at Tevatron for $\sqrt{s} = 1.96 \text{ TeV}$ are [10]

$$\sigma_{\text{exp}} = 7.02 \pm 0.63 \text{ pb} \quad (\text{CDF} : m_t = 175 \text{ GeV}) \quad (24)$$

$$= 8.18^{+0.98}_{-0.87} \text{ pb} \quad (\text{D0} : m_t = 170 \text{ GeV}) : \quad (25)$$

We could decrease the uncertainty if we combined them according to the standard formula of statistics, and indeed such averaging is often seen in many papers. We, however, would rather stay conservative and do not follow this way because it is not easy to treat (average) properly systematic errors in different detectors. In addition, different values are used for m_t in their analyses, which also makes the averaging difficult. At any rate, the uncertainties of CDF and D0 data were $+3.6\% = 2.4 \text{ pb}$ and 2.2 pb respectively when Haberlet al. performed the analysis [6], which tells us that it is truly the time to revisit this analysis.

On the other hand, the total cross section in the framework of QCD with higher order corrections has been studied in detail in [11] (see also [12]). We take the results using the latest set of parton-distribution functions "CTEQ 6.6M" (NNLO approximation) [13]

$$\sigma_{\text{QCD}} = 6.73^{+0.51}_{-0.46} \text{ pb} \quad (m_t = 175 \text{ GeV}) \quad (26)$$

$$= 7.87^{+0.60}_{-0.55} \text{ pb} \quad (m_t = 170 \text{ GeV}) ; \quad (27)$$

and combine these theoretical errors with the above experimental errors as

$$\sigma_{\text{exp}} = 7.02^{+0.81}_{-0.78} \text{ pb} \quad (\text{CDF} : m_t = 175 \text{ GeV}) \quad (28)$$

$$= 8.18^{+1.15}_{-1.03} \text{ pb} \quad (\text{D0} : m_t = 170 \text{ GeV}) : \quad (29)$$

Comparing them with our calculations $(d_V; d_A)$, which is the sum of the central values of the above σ_{QCD} and the non-SM part of our cross sections at the lowest order of perturbation, we find that $d_{V,A}$ are restricted as

$$-0.01 < d_V < +0.01 \quad +0.38 < d_A < +0.41 \quad (30)$$

when we put $d_A = 0$. Similarly we have

$$|d_A| < +0.12 \quad (31)$$

when we put $d_V = 0$. Here, since $(d_V; d_A)$ depends on not d_A but d_A^2 as is known from eqs.(11) and (12), we only get constraints on $|d_A|$. Finally, when we keep both d_V, d_A non-zero, these two parameters produce corrections which tend to cancel each other unless $|d_V|$ is not that sizable, and consequently rather large d_V, d_A are allowed:

$$d_V \approx \pm 0.2 \quad \text{and} \quad |d_A| \approx \pm 0.3: \quad (32)$$

We show the experimentally allowed d_V, d_A region in Fig.3. We find that there still remains some area for these anomalous-coupling parameters, though the standard-model (QCD) prediction, i.e., $d_V, d_A = 0$ is consistent with the data, too.

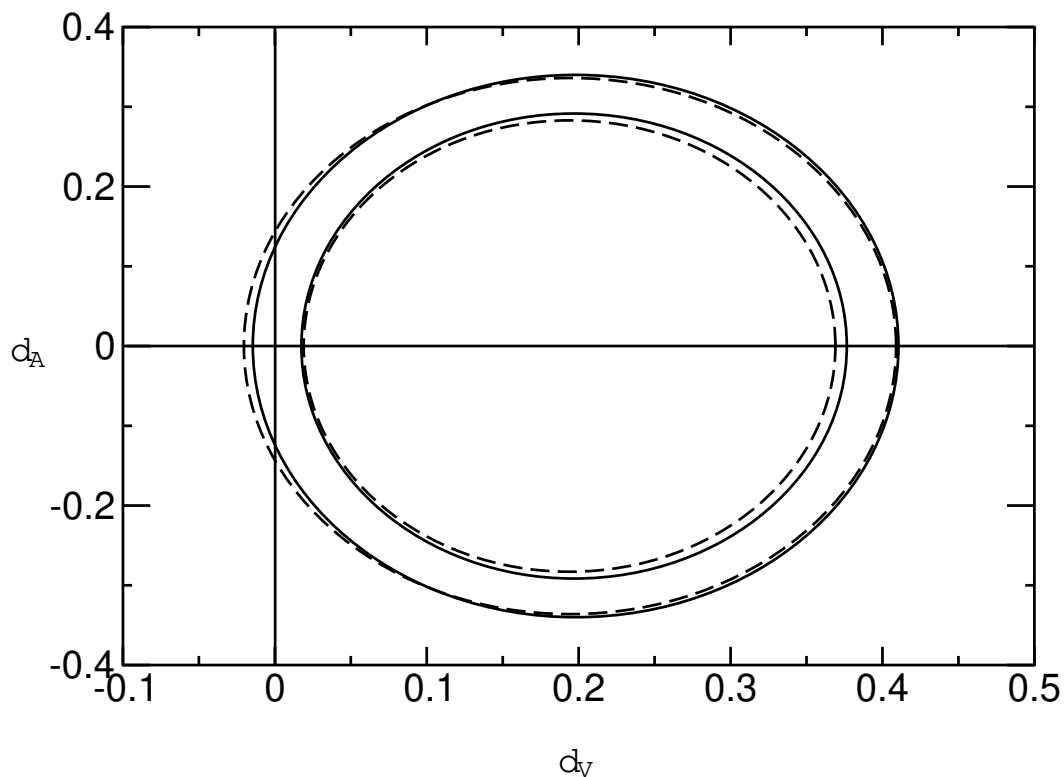


Figure 3: Experimentally allowed region for d_V, d_A . The region between two solid/dashed curves is from CDF/D0 data.

3.2. LHC I: Total cross sections

Let us compute the total cross section and the differential distributions of $pp \rightarrow t\bar{t}X$ at LHC energy ($\sqrt{s} = 10$ and 14 TeV) for

$$(d_V; d_A) = (a) (0.01; 0), (b) (0.41; 0), (c) (0; 0.12), (d) (0.2; 0.3)$$

as typical examples. Concerning the top-quark mass, we use the present world average $m_t = 172$ GeV [14].

First, the total cross sections of top pair productions are:

$$\sqrt{s} = 10 \text{ TeV}$$

$$\begin{aligned} (a) \quad d_V = 0.01; d_A = 0 &= 447 \text{ pb} \\ (b) \quad d_V = 0.41; d_A = 0 &= 1240 \text{ pb} \\ (c) \quad d_V = 0; d_A = 0.12 &= 637 \text{ pb} \\ (d) \quad d_V = 0.2; d_A = 0.3 &= 1835 \text{ pb} \end{aligned} \quad (33)$$

$$\sqrt{s} = 14 \text{ TeV}$$

$$\begin{aligned} (a) \quad d_V = 0.01; d_A = 0 &= 991 \text{ pb} \\ (b) \quad d_V = 0.41; d_A = 0 &= 3479 \text{ pb} \\ (c) \quad d_V = 0; d_A = 0.12 &= 1458 \text{ pb} \\ (d) \quad d_V = 0.2; d_A = 0.3 &= 4744 \text{ pb} \end{aligned} \quad (34)$$

They are much larger than the latest QCD predictions [11]

$$\begin{aligned} \sigma_{\text{QCD}}(\sqrt{s} = 10 \text{ TeV}) &= 415^{+34}_{-29} \text{ pb;} \\ \sigma_{\text{QCD}}(\sqrt{s} = 14 \text{ TeV}) &= 919^{+76}_{-55} \text{ pb;} \end{aligned}$$

In particular, the result with $(d_V; d_A) = (0.2; 0.3)$ is several times larger than σ_{QCD} , which means that we might encounter a surprising observation at LHC.

It is indeed remarkable that the present Tevatron data still allow such a huge cross section at LHC, but this also indicates that coming measurements at LHC might give us a much stronger constraint on $d_{V,A}$. In order to see this possibility clearly, we assume that we have

$$\begin{aligned} \sigma(\sqrt{s} = 10 \text{ TeV}) &= 415 \pm 100 \text{ pb;} \\ \sigma(\sqrt{s} = 14 \text{ TeV}) &= 919 \pm 100 \text{ pb} \end{aligned}$$

at LHC (including possible theoretical uncertainties), and draw figures similar to Fig.3 in Figs.4 & 5. They show that LHC will actually give a very good opportunity to perform precise analyses of top-gluon couplings.

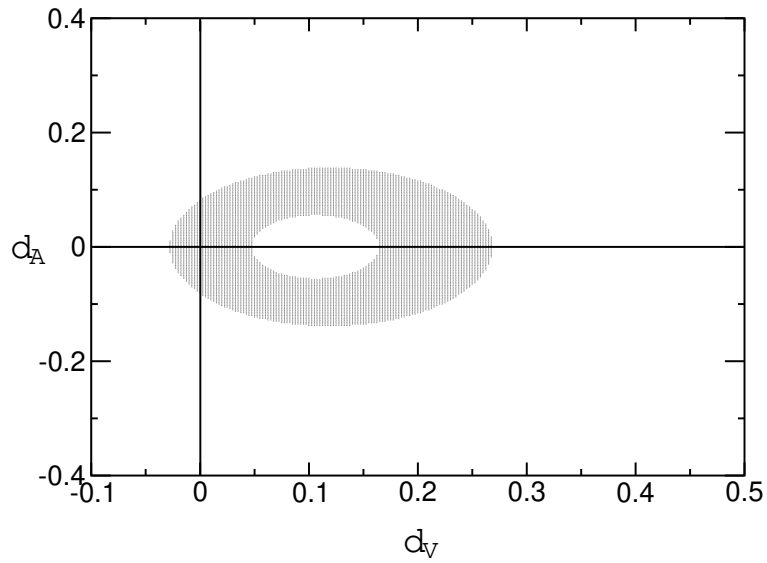


Figure 4: A allowed region for $d_{V,A}$ which LHC ($\sqrt{s} = 10 \text{ TeV}$) might give us.

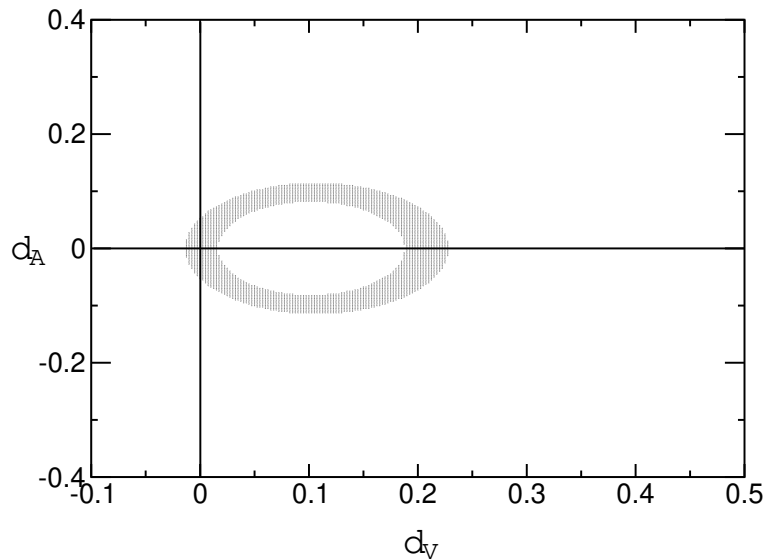


Figure 5: A allowed region for $d_{V,A}$ which LHC ($\sqrt{s} = 14 \text{ TeV}$) might give us.

In this virtual analysis, however, one may expect that $d_V \neq d_A \neq 0$, i.e., an area around the QCD prediction is chosen as the best and unique solution since we used the very QCD result for the central value of the assumed data, but what the two figures show us seems to be against this expectation. This is due to the cancellation between the d_V and d_A terms as mentioned in the previous subsection. Then, is

it is possible to single out QCD even if we got much more precise data as long as we rely on the total cross section alone? Fortunately it is not right: superposing the constraints from Tevatron and LHC, we find that only a small region around $d_V = d_A = 0$ would survive as in Fig.6 if the above assumed LHC data were true.

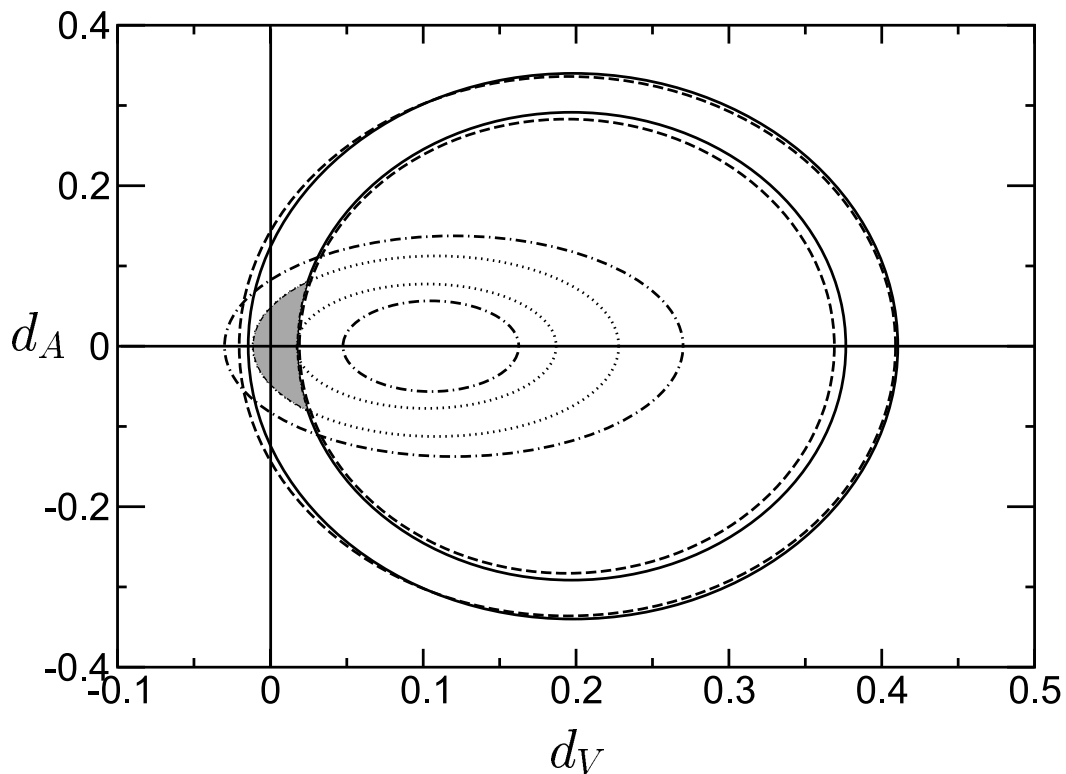


Figure 6: The $d_{V,A}$ region allowed by Tevatron and assumed LHC data (the shaded part).

3.3. LHC II: Differential distributions

Next, we give the top angular distributions in $pp \rightarrow t\bar{t}X$ normalized by $\sigma_0 = \sigma(d_V = d_A = 0)$, i.e., $\frac{1}{\sigma_0} \frac{d\sigma}{d\cos\theta_t}$ in Figs.7 and 8 for $\sqrt{s} = 10$ TeV and 14 TeV, where both d and σ_0 are the tree-level quantities (concerning this approximation, see the later comments). As was just shown, the size of the cross section becomes larger when $d_{V,A} \neq 0$, so the corresponding distributions normalized by σ_0 also

exceed the QCD result (solid curve), and moreover their shapes are different from the QCD distribution.

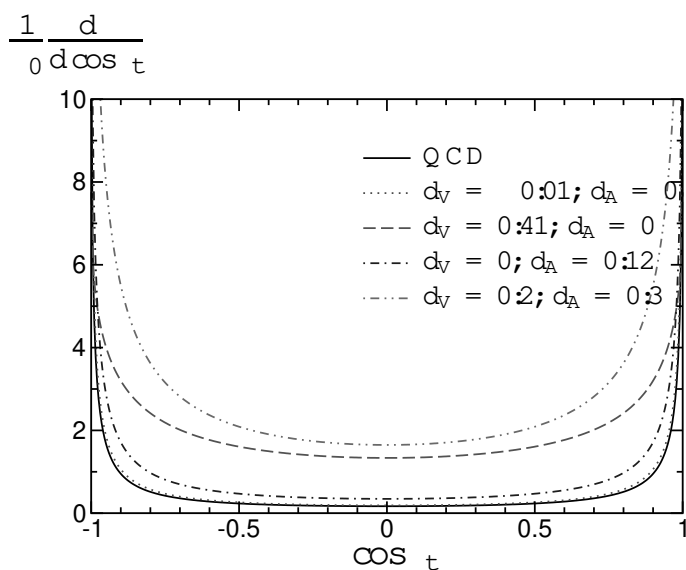


Figure 7: The top angular distribution normalized by d_0 : LHC energy $\sqrt{s} = 10$ TeV

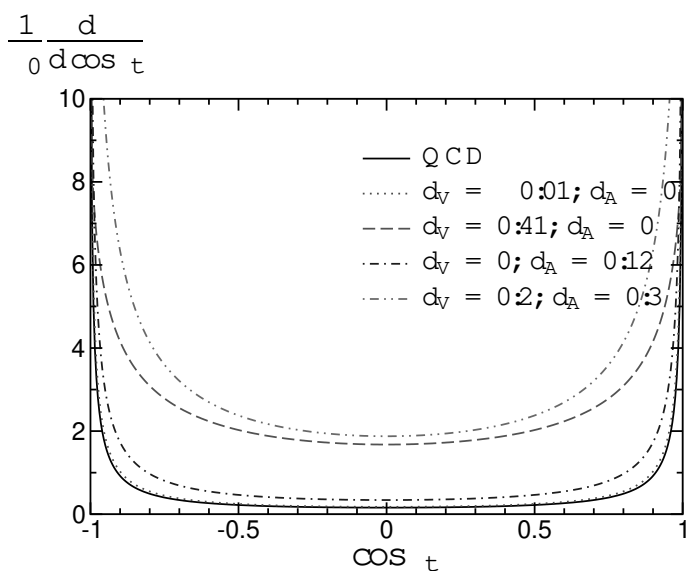


Figure 8: The top angular distribution normalized by d_0 : LHC energy $\sqrt{s} = 14$ TeV

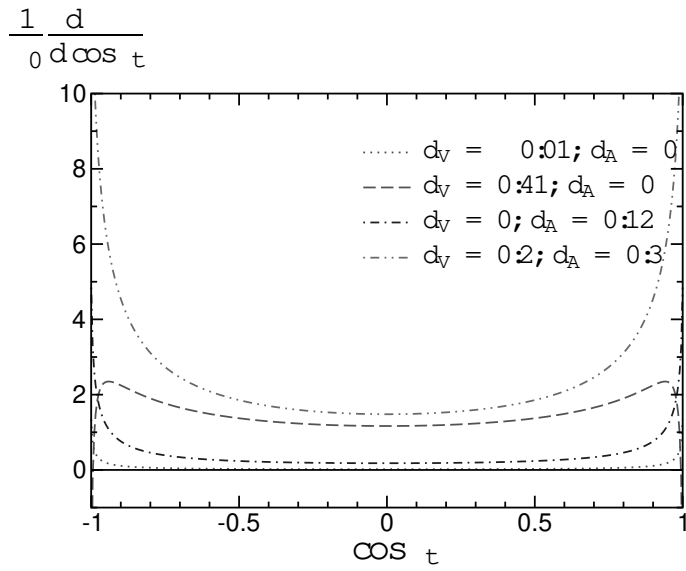


Figure 9: Nonstandard effects in the top angular distribution normalized by d_0 : LHC energy $\sqrt{s} = 10 \text{ TeV}$

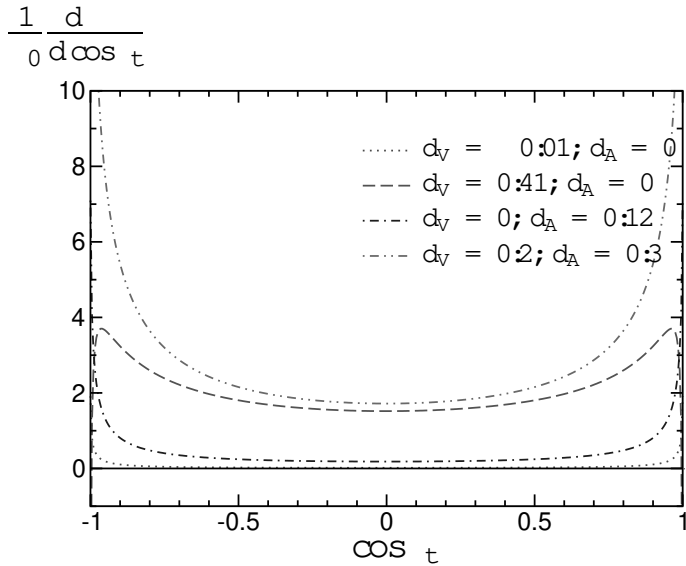


Figure 10: Nonstandard effects in the top angular distribution normalized by d_0 : LHC energy $\sqrt{s} = 14 \text{ TeV}$

Here some comments are necessary about the QCD radiative corrections. We calculated these distributions at the lowest order in perturbation, assuming that most part of the corrections to the standard-model cross sections d_0 is canceled through the normalization between the numerator and denominator, like the au-

thors of [6] did. According to [15], however, we should not rely on this approximation too much. Therefore, we also show in Figs.9 & 10 the pure nonstandard contribution $d_0(d_V; d_A) = d_0$, where we normalize them by the same lowest-order d_0 so that we can directly compare Figs.7 & 8 and Figs.9 & 10. We find that all the curves there are similar to those in the previous figures except that the curve for $d_V = 0.41$ and $d_A = 0$ (the dashed curve) behaves differently when $|\cos \theta_t|$ gets close to 1.

In the same way, let us show the top p_T distributions $d_0^{-1} d = dp_T$ in Figs.11 & 12. There we give the whole distributions alone, not the pure nonstandard contribution to them, since the above figures on the angular distributions told us that the difference is not that significant. We find that the shapes of four curves look rather alike, but the one for $(d_V; d_A) = (0.41; 0)$ behaves differently and therefore apparently distinguishable from the others. In contrast to it, the difference between the QCD curve and the one for $(d_V; d_A) = (0.01; 0)$ is so small that it will be hard to draw meaningful information.

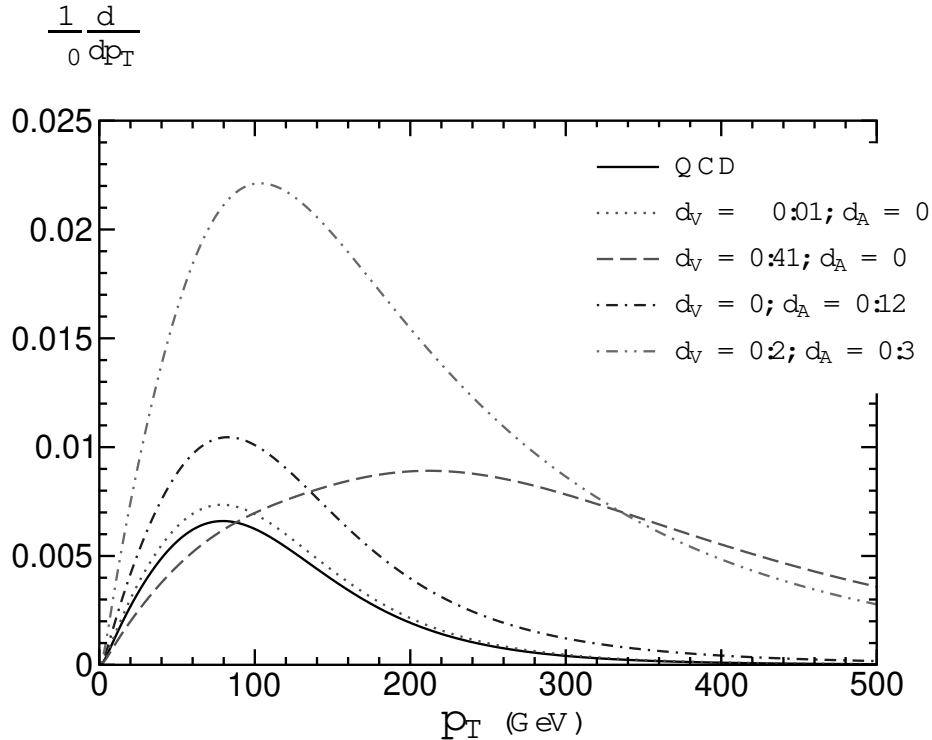


Figure 11: The top p_T distribution normalized by d_0 : LHC energy $\sqrt{s} = 10$ TeV

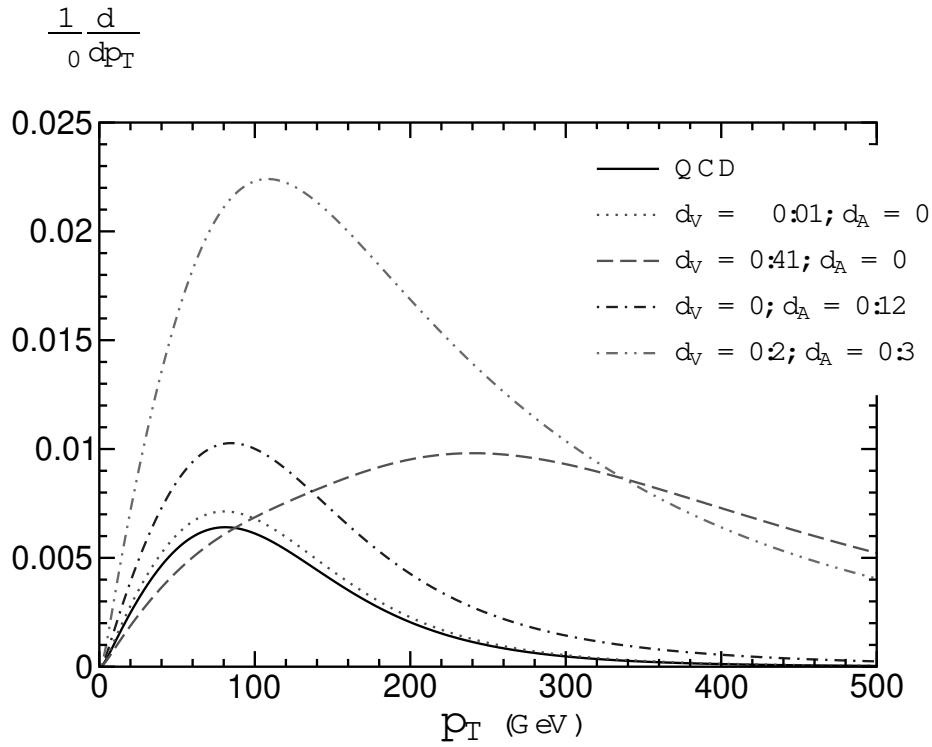


Figure 12: The top p_T distribution normalized by d_0 : LHC energy $\sqrt{s} = 14 \text{ TeV}$

Finally, figures 13 and 14 are the $t\bar{t}$ invariant-mass distributions $d_0^1 d = d_{t\bar{t}}$. Here again the one for $(d_V; d_A) = (0.41; 0)$ behaves a bit differently, and the others will also be usable for our analysis except for $(d_V; d_A) = (0.01; 0)$.

It is not surprising that both the p_T and $t\bar{t}$ invariant-mass distributions for $(d_V; d_A) = (0.41; 0)$ have their peaks at a higher $p_T = p_{t\bar{t}}$ point than the other curves. This is because $d_{V;A}$ terms can be enhanced by the top energy as understood in $M_{q\bar{q}gg}$, and also there occurs partial cancellation between the d_V and d_A contributions when they take similar non-zero values like $(d_V; d_A) = (0.2; 0.3)$, as mentioned in the discussion of the total cross section. This is interesting particularly for the invariant-mass distribution: this is a mere delta-function distribution in the parton-CM frame since $p_{t\bar{t}} = 2E_t = \sqrt{s}$ in this frame. Therefore, we may say that we are observing in figs.13 and 14 the boost effects coming from the parton distribution functions, but still the above enhancement produces some difference.

As a result, we may conclude our analyses as follows: those three differential distributions seem to indicate that there will be some chances to observe anomalous-coupling effects unless $|d_{V;A}|$ is very small, although their effects are not as drastic

in these quantities as in the total cross section.

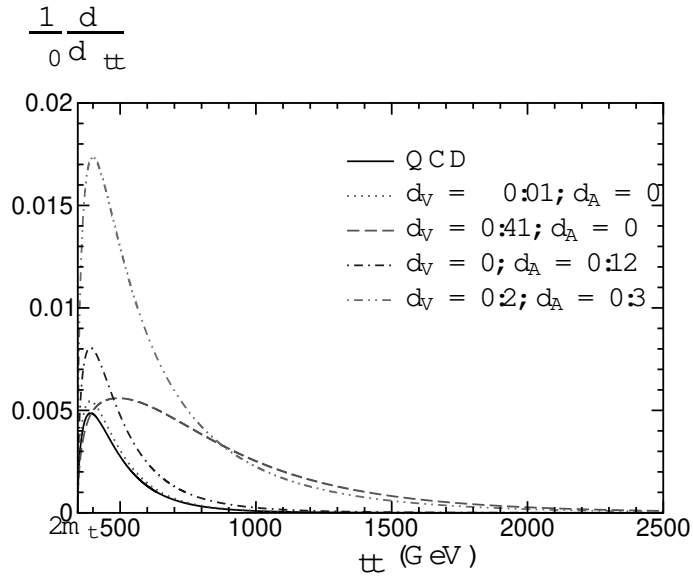


Figure 13: The $t\bar{t}$ invariant-mass distribution normalized by σ_0 : LHC energy $\sqrt{s} = 10$ TeV

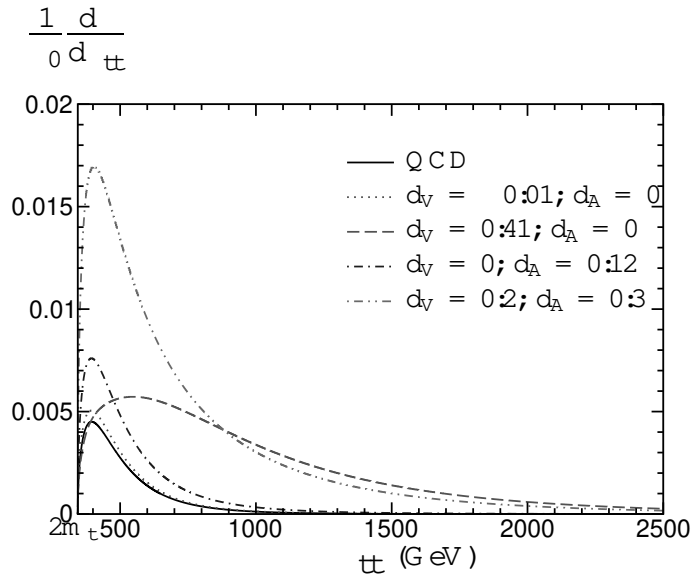


Figure 14: The $t\bar{t}$ invariant-mass distribution normalized by σ_0 : LHC energy $\sqrt{s} = 14$ TeV

4. Summary

We have studied in this article anomalous top-gluon coupling effects in the total cross section and several differential distributions of $pp \rightarrow t\bar{t}X$ at LHC energies

$\sqrt{s} = 10$ and 14 TeV in the framework of dimension-6 effective operators. We first obtained an experimentally allowed region for the chromoelectric and chromomagnetic moments from Tevatron (CDF/D0) data on the total cross section of $pp \rightarrow t\bar{t}X$, then we thereby computed the above-mentioned quantities.

We found the total cross section could get much larger than the standard-scheme (QCD) prediction. Also the top distributions could show a different behavior from QCD, though the non-SM effects are not as drastic as in the total cross section. It must be quite exciting if we actually get a huge cross section at LHC. Conversely, if we observe cross section close to the QCD prediction, we obtain a much stronger constraint on d_V and d_A . In that case, an analysis combining the Tevatron and LHC data will work very effectively.

We focused here on the top quark itself in the final state, and did not go into detailed analyses of its various decay processes, since it would help to maximize the number of events necessary for our studies. Indeed we have thereby shown that there would be some chances to observe interesting phenomena. However, if we get any nonstandard signal, we of course have to perform more systematic analyses including decay products, i.e., leptons/b quarks. We should get ready for such an exciting situation as a next subject before actual experiments start.

ACKNOWLEDGMENTS

The algebraic calculations using FORM were carried out on the computer system at Yukawa Institute for Theoretical Physics (YITP), Kyoto University.

Note added

After the completion of this work, we were informed that anomalous top-gluon couplings were also studied in [16] to explore the possibility that the right-handed top quark is composite. We would like to thank Tim Tait for calling our attention to these two papers.

REFERENCES

[1] LHC web-site: <http://public.web.cern.ch/public/en/LHC/LHC-en.html>

- [2] W. Buchmüller and D. Wyler, Nucl. Phys. B 268 (1986) 621.
C. Arzt, M. B. Einhorn and J. Wudka, Nucl. Phys. B 433 (1995) 41
(hep-ph/9405214).
- [3] B. Grzadkowski, Z. Hlengi, K. Ohkuma and J. Wudka, Nucl. Phys. B 689
(2004) 108 (hep-ph/0310159).
- [4] J.A. Aguilar-Saavedra, Nucl. Phys. B 812 (2009) 181 (arXiv:0811.3842 [hep-ph]); arXiv:0904.2387 [hep-ph].
- [5] CDF collaboration: <http://www-cdf.fnal.gov/>
D0 collaboration: <http://www-d0.fnal.gov/>
- [6] P. Haberl, O. Nachtmann and A. Wilch, Phys. Rev. D 53 (1996) 4875
(hep-ph/9505409).
- [7] D. Atwood, A. Appel and A. Soni, Phys. Rev. Lett. 69 (1992) 2754.
A. Brandenburg and J.P. Ma, Phys. Lett. B 298 (1993) 211.
D. Atwood, A. Kagan and T.G. Rizzo, Phys. Rev. D 52 (1995) 6264
(hep-ph/9407408).
K. Cheung, Phys. Rev. D 53 (1996) 3604 (hep-ph/9511260).
D. Silverman, Phys. Rev. D 54 (1996) 5563 (hep-ph/9605318).
K. Whisnant, J.M. Yang, B.L. Young and X. Zhang, Phys. Rev. D 56 (1997)
467 (hep-ph/9702305).
J.M. Yang and B.L. Young, Phys. Rev. D 56 (1997) 5907 (hep-ph/9703463).
S.Y. Choi, C.S. Kim and J. Lee, Phys. Lett. B 415 (1997) 67
(hep-ph/9706379).
B. Grzadkowski, B. Lampe and K.J. Abraham, Phys. Lett. B 415 (1997) 193
(hep-ph/9706489).
B. Lampe, Phys. Lett. B 415 (1997) 63 (hep-ph/9709493).
K.I. Hikasa, K. Whisnant, J.M. Yang and B.L. Young, Phys. Rev. D 58 (1998)
114003 (hep-ph/9806401).
H.Y. Zhou, Phys. Rev. D 58 (1998) 114002 (hep-ph/9805358).
J. Splin, J. Phys. G 29 (2003) 543.
O. Antipin and G. Valencia, Phys. Rev. D 79 (2009) 013013 (arXiv:0807.1295

[hep-ph]).

S.K. Gupta, A.S.Mete and G.Valencia, arXiv:0905.1074 [hep-ph].

For a related review, see:

D.A. Atwood, S.Bar-Shalom, G.Eilam and A.Soni, Phys.Rept. 347 (2001) 1 (hep-ph/0006032).

[8] J.A.M. Vermaseren, "Symbolic Manipulation with FORM", version 2, Tutorial and Reference Manual, CAN, Amsterdam 1991, ISBN 90-74116-01-9.

[9] M.Gluck, J.F.Owens and E.Reya, Phys.Rev.D 17 (1978) 2324.

B.L.Combridge, Nucl.Phys.B 151 (1979) 429.

[10] CDF collaboration: Public CDF note 9448 (http://www-cdf.fnal.gov/physics/new/top/public_xsection.html).

D0 Collaboration: V.M.Abazov et al., arXiv:0903.5525 [hep-ex].

[11] N.Kidonakis and R.Vogt, Phys.Rev.D 78 (2008) 074005 (arXiv:0805.3844 [hep-ph]).

[12] S.Moch and P.Uwer, Phys.Rev.D 78 (2008) 034003 (arXiv:0804.1476 [hep-ph]).

M.Cacciari, S.Frixione, M.L.Mangano, P.Nason and G.Ridol, JHEP 0809, 127 (2008) (arXiv:0804.2800 [hep-ph]).

[13] P.M.Nadolsky et al., Phys.Rev.D 78 (2008) 013004 (arXiv:0802.0007 [hep-ph]).

[14] Tevatron Electroweak Working Group for the CDF and D0 Collaborations, arXiv:0808.1089 [hep-ex].

[15] W.Beenakker, W.L.van Neerven, R.Meng, G.A.Schuler and J.Smith, Nucl.Phys.B 351 (1991) 507.

[16] B.Lillie, J.Shu and T.M.P.Tait, JHEP 0804 (2008) 087 (arXiv:0712.3057 [hep-ph]).

K.Kumar, T.M.P.Tait and R.Vega-Morales, JHEP 0905 (2009) 022 (arXiv:0901.3808 [hep-ph]).